ISOMAse
International Society of Ocean, Mechanical and Aerospace Scientists and Engineers

Journal of Ocean, Mechanical and Aerospace
-Science and Engineering-
30th November 2023. Vol.67 No.3

November 30, 2023

Development of Rotary Fatigue Test Equipment Based on the Joseph Marin Approach

Anang Prasetyo[a], Efi Afrizal[b]* and Nazaruddin[b]

a) *Master Student in Mechanical Engineering, Universitas Riau, Indonesia*
b) *Mechanical Engineering Department, Universitas Riau, Indonesia*

*Corresponding author: efiafrizal@lecturer.unri.ac.id

Paper History

Received: 07-October-2022
Received in revised form: 15-May-2023
Accepted: 30-November-2023

ABSTRACT

This paper proposed the development of rotary fatigue test equipment. This equipment was used to test the JIS S45C steel, validated using the Joseph Marin approach. Analyzing the fatigue strength of JIS S45C steel using the Joseph Marin approach was compared to experimental testing. The dimension of the test specimens was based on the ASTM E 466. The test data was displayed in the form of an S-N curve. The test results showed the fatigue strength of JIS S45C steel on the whole that was close to each other, experimentally and using the Joseph Marin approach. In the infinite life region, it is known that the fatigue strength based on the Joseph Marin approach was lower than experimental tests. Therefore, if JIS S45C steel had received a hefty load repeatedly, it would fail more quickly.

KEY WORDS: *Fatigue test equipment, JIS S45C steel, Joseph Marin approach, Specimen.*

NOMENCLATURE

N	*Fatigue cycle*
σ_{yield}	*Percentage of yield load*
σ_f	*Fracture*
F	*Force*
$\sigma_{bending}$	*Bending stress*
T_{shear}	*Shear stress*
W	*Weight*
F_F	*Friction Force*
ε_{sd}	*Compressive strain*
ε_c	*Critical strain*

1.0 INTRODUCTION

In the world of fabrication, knowledge of materials science is closely related to the process of designing products that will be produced. Creating new products will begin with designing products that the company can sell to consumers. In the production process, the primary role is owned by the designer as the generation of ideas, concept development, testing and implementation of manufacturing physical objects or services. Tool development is carried out by looking for more complex problems. The designers can determine the dimensions and types of materials used by considering the ease of making product designs to minimize costs [1-2]. Thus, simplifying the manufacturing process and minimizing the risk of errors and repetitive work [3].

The mechanical properties of steel have a crucial role that can be applied for use in the field by effective use and efficiency [4-5]. Most steels are subjected to dynamic and repeated stress loading over a long time, resulting in curvature stress whose magnitude varies continuously from the maximum compressive value to the maximum tensile value. This tensile pull condition lasts continuously until the material is tired and ends with a fracture or fatigue failure. The fatigue life determines the load cycles before failure [6]. Fatigue failure occurs based on the endurance limits of a material. Fatigue problems often arise and are difficult to estimate, with no signs of fatigue fractures that can be seen with the naked eye during work in the field by technicians in each field [7-8].

Some materials can experience repeated stresses or fluctuations that can cause damage below the stress required to break tired, with dynamic loading resulting in cracks that can propagate continuously, resulting in the strength and ductility of a structure decreasing lower than the load that must be supported. As a result, the structure cannot withstand the load, failing [9-13]. The use of steel specimens can be very different compared to other regions, so it is necessary to pay attention to the strength of the steel [14]. It is necessary to investigate the properties of a material by testing using fatigue test equipment. However, due to the limited accuracy of existing fatigue test equipment in the form of a loading system that is directly not accompanied by a load gauge and the inaccuracy of cycle results because the system stops manually and the surface of

ISOMAse International Society of Ocean, Mechanical and Aerospace Scientists and Engineers
Journal of Ocean, Mechanical and Aerospace
-Science and Engineering-
30th November 2023. Vol.67 No.3

November 30, 2023

the fault results rubs against each other [15].

Thus, this paper aims to develop a rotary bending fatigue test equipment. Some improvements were made, such as changing manual components to digital in motor rotation measuring instruments (rpm), time (minutes), arm loading systems, load counters, and automatic stop systems. So, it can be ensured that the broken surfaces on the test specimens do not rub against each other. Thus, the shape of the fault that occurs can be analyzed. The test results are displayed as an S–N (fatigue) diagram. The result data is displayed more proportionally attractively, making it easier for the structural designer. In addition, this rotary fatigue test equipment can be applied to testing other materials such as aluminum, copper, composites and others.

2.0 METHODOLOGY

The development of rotary fatigue test equipment involved the design and manufacturing of the equipment frame, motor drive mount, and rotation transmission system to the shaft, shaft, shaft bearing base, and designing tools for measuring motor rotation (rpm), time (minutes), load distribution system, tools measuring loads, automatic stop systems, electrical and control systems. This test equipment used the digital system with the addition of an Arduino tool as a controller to measure rotation, time and automatic shutdown. Arduino is an electronic board that functions as a computer to control the operation [16-17] of rotary fatigue test equipment. In the form of calculating the number of revolutions, calculating the time, on, off, restart, and stopping automatically when the test specimen breaks. In this paper, the control system used an Arduino Atmega 328 microcontroller. The data generation for fatigue testing equipment was displayed on the LCD screen. The Arduino circuit design is shown in Figure 1.

The rotary fatigue test equipment design is depicted in Figure 2. The working principle of the equipment was the control system turned on, which automatically started the motor. Next, the motor rotation was transferred to the shaft via pulley and belting. So, the specimen gripped by the collet rotated at a speed of 870 rpm and received the bending stress. The specimens that had received bending stress would experience repeated stress due to torsion. With continuous loading in specific cycles, the specimen can break. When the specimen breaks, the motor is automatically stopped, and the rotation results and time are displayed on the LCD screen. Next, a reset was carried out to test the next specimen.

Next, the rotary fatigue test equipment carried out fatigue testing for JIS S45C material specimens. The tensile testing was carried out to obtain the yield strength value. According to [18-19], fatigue is a form of structural failure due to dynamic loads that fluctuate below yield strength and occur for a long time and repeatedly. In this research, the fatigue test was carried out with JIS S45C steel specimens by conducting tensile testing. To obtain yield strength values were used to vary the loads 50%, 70%, 90%, 110% and 130%, which obtained the load applied to the fatigue test equipment along with ASTM E-8 standard for tensile test of specimen sizes (Figure 3) and fatigue test specimen sizes (Figure 4).

Data from each test specimen on JIS S45C steel with varying loads was collected to determine the specimen operating cycle. The magnitude of the working stress due to loading and testing cycles was a reference for numerically determining the number of cycles. Other predictions were approached using Joseph Marin's equation.

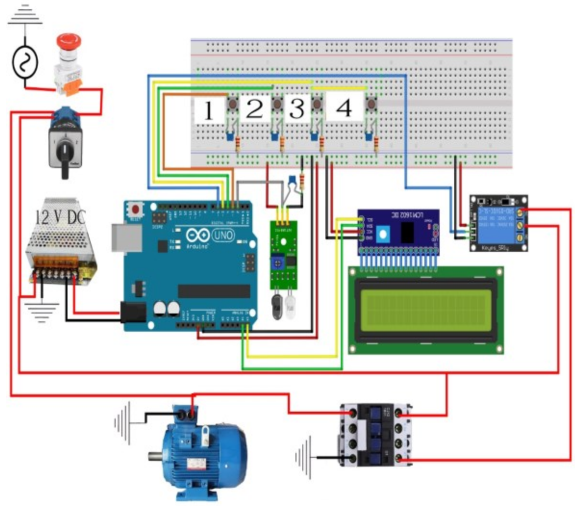

Figure 1: Arduino control system circuit

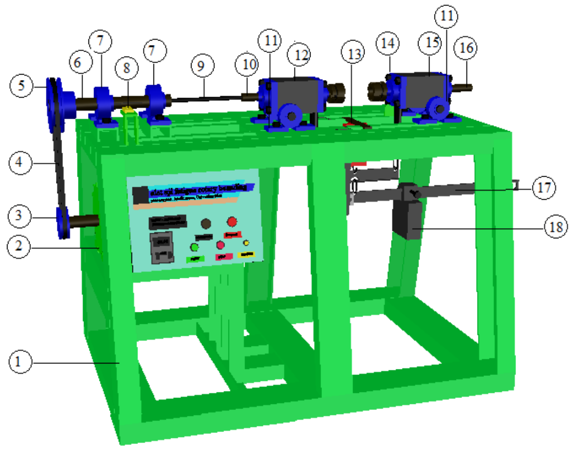

Note:

1. Construction of frames
2. Electric motor
3. Drive motor pully
4. Belting
5. Shaft connecting pully
6. Shaft
7. Bearing UCP 1
8. *IR* Round counter
9. Flexible cable
10. Chuck shaft 1
11 Bearing UCP 2
12. Arm shaft position box 1
13. Weight gauge
14. Lap and time stop switch
15. Arm shaft position box 1
16. Chuck shaft
17 Loading arm.
18 Control the amount of loading

Figure 2: Rotary fatigue test equipment design

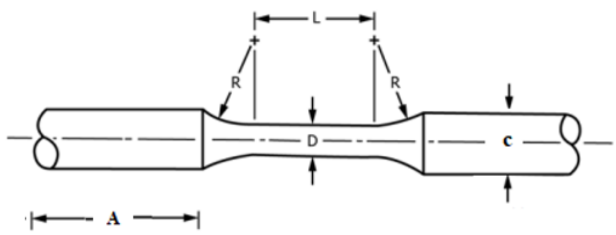

A = 60; D = 9; C = 15; L = 45; R = 45

Figure 3: Specific size for tensile test specimen [20]

JOMAse | Received: 07-October-2022 | Accepted: 30-November-2023 | [(67) 3: 95-100]
Published by International Society of Ocean, Mechanical and Aerospace Scientists and Engineers, www.isomase.org., ISSN: 2354-7065 & e-ISSN: 2527-6085

ISOMAse
International Society of Ocean, Mechanical and Aerospace Scientists and Engineers
Journal of Ocean, Mechanical and Aerospace
-Science and Engineering-
30th November 2023. Vol.67 No.3

November 30, 2023

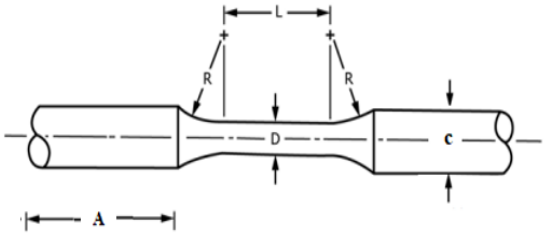

D = 6 mm; C = 14 mm; L = 18 mm; A = 24 mm; R = 48 mm.

Figure 4: The size of fatigue test specimens [21]

3.0 RESULTS AND DISCUSSION

The stages of designing and manufacturing the rotary fatigue test equipment first inspect the previous equipment and redesign the rotary fatigue test equipment, including designing the construction, shafts, bearings, couplings, electrical circuits and controls using the Arduino program. The rotating fatigue test equipment is shown in Figure 5.

Figure 5: The rotary fatigue test equipment

3.1 The Rotary Fatigue Test Equipment Examining

Fatigue testing was carried out with JIS S45C steel material with a yield strength of 500.86 MPa from the tensile test results, as presented in Table 1 and Figure 6 as a JIS S45C steel tensile test graph. JIS S45C steel was tested by varying the load of 50%, 70%, 90%, 110% and 130% of the yield strength. The load given to the specimen is presented in Table 1. The tensile testing can be seen in Figure 7.

Determining the load given in the fatigue testing of the JIS S45C material refers to the yield strength results of 500.86 MPa. The dimensions of the test specimen are shown in Figure 4. Based on equation (1), the load for fatigue testing on each specimen. Then, the load applied in each specimen is shown in Table 2.

Table 1: JIS S45C steel tensile test result

No	Result	Value
1	Yield strength	500.86 MPa
2	Ultimate tensile strength	806.39 MPa
3	Ɛ (%)	7.133
4	σf	610.069 MPa

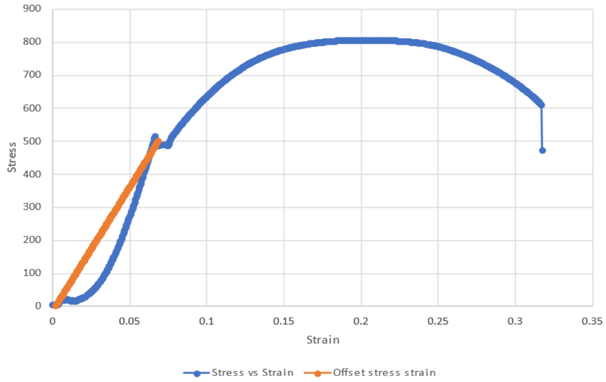

Figure 6: Stress vs Strain Curve

Figure 7: Tensile testing

$$\sigma_{yield} = \frac{w.l/2}{\pi/32.d^3} \quad (1)$$

$$\frac{w.100}{2} = (500{,}86 \times 50\%).(\pi/32.(6^3))$$

w = 106.16N

w = 10.9 Kg

Table 2: Loading value of each specimen

No	Specimen data	Percentage %	Load (kg)
1	Specimen 1	50	10.9
2	Specimen 2	70	15.9
3	Specimen 3	90	19.9
4	Specimen 4	110	23.9
5	Specimen 5	130	28.9

3.2 Bending Stress

The bending stress for each specimen was calculated based on data of specimen diameter of 6 mm and gravity (g) of 9.81 m/dt^2. The size of specimen shows in Figure 8.

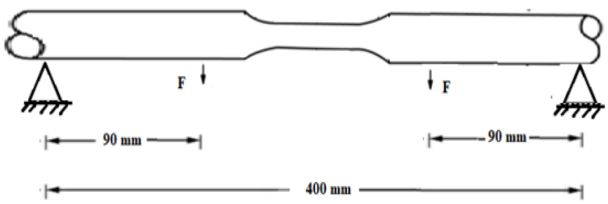

Figure 8: The specimen size for bending stress

JOMAse | Received: 07-October-2022 | Accepted: 30-November-2023 | [(67) 3: 95-100]
Published by International Society of Ocean, Mechanical and Aerospace Scientists and Engineers, www.isomase.org., ISSN: 2354-7065 & e-ISSN: 2527-6085

Journal of Ocean, Mechanical and Aerospace
-Science and Engineering-
30th November 2023. Vol.67 No.3

Specimen 1, with a load of 10.9 kg, was calculated as the force:

Force (F) = Mass x gravity
= 5.45x 9.81 m/dt^2
= 53.464 N

Determining the bending stress can be calculated using equation (2). Then, the bending stress value calculation resulted in 2.2 x108 N/m² = 227.03 MPa. The same way was applied to calculate the bending stress for specimens two to 5.

$$\sigma = \frac{M.y}{I} = \frac{F.l.\frac{1}{2}.d}{\frac{\pi.d^4}{64}} \qquad (2)$$

3.3 Shear Stress

The following equation can obtain the shear stress on the specimen:

$$\tau_{Shear} = \frac{T.r}{I_p} \qquad (3)$$

Then, the shear stress for specimens 1 to 5 was calculated using equation (3). The result of the bending and shear stress values for all specimen tests is depicted in Table 3.

Table 3: Bending and shear stresses acted in each specimen

No	Load % Yield	Specimen load	Bending stress (Mpa)	Shear stress (Mpa)
1	50%	10.9	227.03	142.41
2	70%	15.9	331.17	142.41
3	90%	19.9	414.48	142.41
4	110%	23.9	497.79	142.41
5	130%	28.9	606.10	142.41

3.4 Fatigue Testing

Fatigue testing of JIS S45C steel used the rotary fatigue test equipment. The fatigue strength result of JIS S45C steel with the fatigue S-N is shown in Figure 8. The formula of cycle (N) was time (minute) multiplied by motor rotation (rpm). The result of the cycle value for specimens one to 5 can be seen in Table 4.

Table 4: The fatigue test results in each specimen

Data Specimen	Tension Max (MPa)	Load % yield	Cycle (N)
Specimen 1	295.63	50%	1,869,795,460
Specimen 2	383.98	70%	495,119,800
Specimen 3	458.69	90%	22,144,683
Specimen 4	535.65	110%	363,581
Specimen 5	637.89	130%	4,883

3.5 Approach Using Joseph Marin

The Joseph Marin was one of the pioneers in the collection, development, and dissemination of material on the failure of engineering elements since 1952 [22]. Fatigue failure is caused by the formation and propagation of cracks [23]. Fatigue cracking is usually begun at a discontinuity in the material where the maximum cyclic stress [24-26], in *Joseph Marin's* approach first determined the fatigue force fraction f, of Sut.

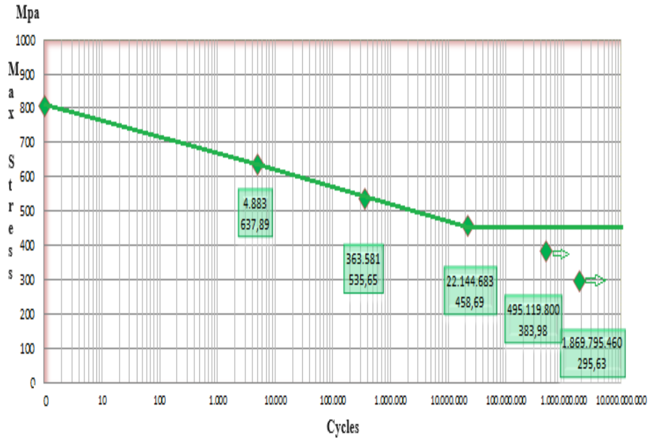

Figure 8: S-N curve result of testing experiment

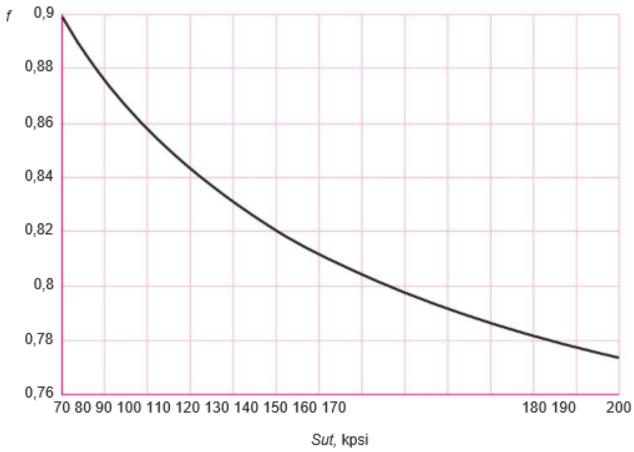

Figure 9: Fatigue strength fraction of f

For actual mechanical components was reduced to Se, which value of less than 0.5 Sut. The recommendation f value was found from Figure 9. Equations (a) and (b), for actual mechanical components, can be written in the following form:

$$a = \frac{(Fs_{ut})^2}{S_e} \qquad (5)$$

$$b = 1/_3 \log\left(\frac{Fs_{ut}}{S_e}\right) \qquad (6)$$

Where N was the cycle to failure and the constants a and b were determined by points 103 and 106, the number of cycles to failure can be expressed by the following equation:

$$\sigma_{af} \geq sf =_a N^b = N\left(\frac{\sigma_{rev}}{a}\right)^{1/b} \qquad (7)$$

Based on *Joseph Marin's* equations (5), (6), and (7) with a tension of 295.63 MPa for specimen 1, then was obtained the cycle (N) of 76.136.711. Hence, the cycle was calculated the same way for specimens two to 5. The cycle value of the manual calculation of *Joseph Marin's* equation can be seen in Table 5. The comparison between the experimental S-N curve and *Joseph Marin's* equation value is shown in Figure 10.

JOMAse | Received: 07-October-2022 | Accepted: 30-November-2023 | [(67) 3: 95-100]
Published by International Society of Ocean, Mechanical and Aerospace Scientists and Engineers, www.isomase.org., ISSN: 2354-7065 & e-ISSN: 2527-6085

Journal of Ocean, Mechanical and Aerospace
-Science and Engineering-
30th November 2023. Vol.67 No.3

November 30, 2023

Table 5: The manual calculation result of cycle used the *Joseph Marin's* equation

No	Tension (MPa)	Cycle
1	295.63	76,136,711
2	383.98	1,975,971
3	403.00	1,005,943
4	458.69	165,033
5	535.65	18,919
6	637.89	1,650
7	661.00	1,004

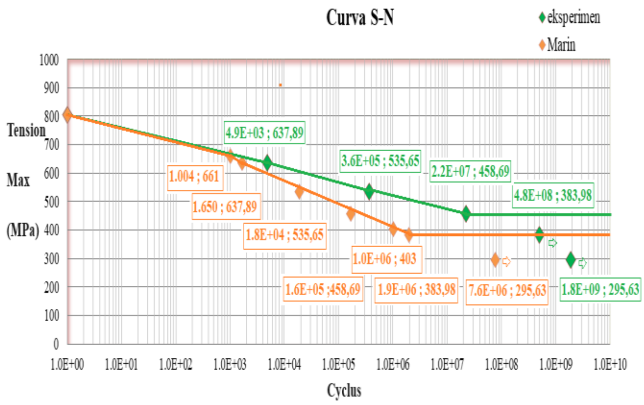

Figure 10:1 The result of the experimental S-N curve versus Joseph Marin's approach

The results of the approach using *Joseph Marin's* equation showed that the more significant load acting on the specimen can accelerate the fatigue life. The smaller the tension on the specimen, the higher the fatigue life. The results shown on specimen 1 with a tension of 295.63 MPa with 76,136,711 cycles. The tension of 637.89 MPa showed the results of 4,883 cycles. The endurance limits with a cycle of 1,005,943 obtained at a tension of 403 MPa. It is also supported by the experimental test result, which showed a tension on specimen 1 of 295.63 MPa, a result of 1,869,795,460 cycles. Specimen 5 has a working tension of 637.89 MPa, showed a result of 4,883 cycles, and obtained endurance limits at a tension of 458.69 MPa with a cycle of 22,144,683. It shows the endurance limits results both in the approach using the *Joseph Marin's* equation and experiments revealed below the yield strength value of JIS S45C steel.

4.0 CONCLUSION

This paper aims to develop rotary fatigue test equipment. The rotary fatigue test equipment was improved by changing manual components to digital in motor rotation measuring instruments (rpm), time (minutes), arm loading systems, load counters, and automatic stop systems. The control system used an Arduino Atmega 328 microcontroller. The data generated for fatigue testing is displayed on the LCD screen. The rotary fatigue test equipment was examined for fatigue testing for the JIS S45C material specimen. JIS S45C steel, with a yield strength of 500.86 MPa and an ultimate tensile strength of 806.39 MPa, was used as a test specimen to prove the performance of rotary bending fatigue test equipment. The fatigue test resulting from the JIS S45C steel has a high cycle fatigue with a cycle of 22,144,683, at a load of 90% of the yield tension or a working tension of 458.69 MPa. The test results and fatigue test calculations of the JIS S45C specimen show that a minor tension can produce a larger fatigue limit, and finally, the test specimen would break. Vice versa at greater tension, resulting in smaller fatigue limits. The infinite-life region or fatigue strength based on Joseph Marin's equation was revealed to be lower than experimental testing. Therefore, the JIS S45C steel, when receiving large enough loads repeatedly, will fail faster.

REFERENCE

[1] Pranata, D. & D.S. Arief (2021). Automatic task machine (atm) design for logistic package by method analytical hierarchy process (ahp) through approach the design for manufacturing (dfm). *Journal of Ocean, Mechanical and Aerospace-science and engineering-*, 65(1), 1-7.

[2] Yunus, N. & Susilawati, A. (2020). Innovation of elbow fixture welding process based on design for manufacture and assembly (DFMA). Journal of Ocean, Mechanical and Aerospace-science and engineering-, 64(1), 19-24.

[3] Hisyam, K.M. & Hamid, A. (2017). Menganalisa pengaruh besar beban lentur terhadap kekuatan fatik poros tembaga. *Zona Mesin*, 8(2).

[4] Wijaya, S. (2018). *Perencanaan Mesin Uji Lelah Rotating Bending untuk Baja Aisi 1045* (Doctoral dissertation, Unimed).

[5] Syukur, M.A. & Carles, H. (2021). Penentuan parameter parameter input proses pemesinan milling dan gurdi untuk pembuatan pencekam spesimen alat uji lelah dengan kekuatan maksimum 370 mpa. *AME (Aplikasi Mekanika dan Energi): Jurnal Ilmiah Teknik Mesin, Universitas Mercu Buana Jakarta*, 7(2), 67-73.

[6] Mujahid, A.S. (2019). Mitigation for Hawser's short fatigue life on the study of the fatigue life prediction of hawser in single point mooring (spm) at Tuban fuel terminal. *Journal of Ocean, Mechanical and Aerospace-science and engineering-*, 63(3), 5-12.

[7] Pratowo, B., et al. (2019). Analisis kekuatan fatik baja karbon rendah sc10 dengan tipe rotary bending. *Jurnal Teknik Mesin, Program Studi Teknik Mesin, Universitas Bandar Lampung (UBL)*, 7(1).

[8] Siregar, A. (2000). *Pengaruh Struktur Mikro Lapisan Chromized pada Baja 42CrM04 Terhadap Kelakuan Fatik*. Fakultas Teknik Universitas Medan Area, Medan.

[9] Hendrawan, B. (2010). *Pengaruh Perbandingan Tegangan (Stress Ratio) Terhadap Laju Perambatan Retak Fatik Panel Komposit Berpenguat Kombinasi Serat Kenaf Anyam dan Kontinyu.* Skripsi Jurusan Teknik Mesin Fakultas Teknik Universitas Sebelas Maret Surakarta.

[10] Suhartono, H.A. (2007). Aplikasi tegangan-regangan ekivalen pada perhitungan umur fatik paduan al 6063 untuk beban aksial dan torsi. *Mesin Balai Besar Teknologi Kekuatan Struktur, UPT LUK BPPT*, 9(1).

[11] Rahmatullah, R. & Ahmad, R. (2018). Analisa pengujian lelah material bronze dengan menggunakan rotary bending fatigue machine. *Jurnal Rekayasa Material, Manufaktur dan Energi*, *1*(1), 1-11.

JOMAse | Received: 07-October-2022 | Accepted: 30-November-2023 | [(67) 3: 95-100]
Published by International Society of Ocean, Mechanical and Aerospace Scientists and Engineers, www.isomase.org., ISSN: 2354-7065 & e-ISSN: 2527-6085

[12] Bahtiar, D. (1997). *Pengaruh Heat Input pada Pengelasan Saw Baja Kekuatan Tinggi Terhadap Perambatan Retak dan Umur Lelah Daerah HAZ.* Doctoral dissertation, Institut Teknologi Sepuluh Nopember.

[13] Fitri, M. (2020). Pengaruh beban lentur pada poros stainless steel terhadap siklus kegagalan fatik. *Jurnal Teknik Mesin Universitas Mercu Buana,* 9(3), 149.

[14] Dalil, M. & Fatra, W. (2011). Pengaruh air gambut terhadap kekuatan lelah baja struktur. *Seminar Nasional Tahunan Teknik Mesin X Tahun 2011 Jurusan Mesin Fakultas Teknik Universitas Brawijaya Malang*.

[15] Kennedy, J. (2010). *Perancangan Dan Pembuatan Alat Uji Fatik Rotating Pure Bending*. Jurusan Teknik Mesin, Fakultas Teknik, Universitas Riau.

[16] Yohanes, Y. & Alqolbi, M.R. (2020). Development of dynamometer based on strain gauge with sensor rod type four square stalk to measuring the drive power of rotary friction welding machine. *Journal of Ocean, Mechanical and Aerospace-science and engineering*-, 64(1), 9-15.

[17] Arief, D.S., et al. (2018). Modeling of control system on sorting palm fruit machine by using arduino microcontroller. *Journal of Ocean, Mechanical and Aerospace-science and engineering*-, 52(1), 1-5.

[18] Astika, I.M. (2009). Karakteristik lelah chopped strand mat/polyester composite. *Jurnal Ilmiah Teknik Mesin*, 9(03), 150.

[19] Budiyanto, E., Nugroho, E. & Zainudin, A. (2018). Uji ketahanan fatik aluminium scrap hasil remelting piston bekas menggunakan alat uji fatik tipe rotary bending. *Turbo J. Progr. Stud. Tek. Mesin*, *7*(1).

[20] ASTM-E8 (2016). Standard test methods for tension testing of metallic materials. *Journal of Testing and Evaluation*, 45(6), 2294-2298.

[21] ASTM-E466 (2020). *Standard Practice for Conducting Force Controlled Constant Amplitude Axial Fatigue Tests of Metallic Materials*.

[22] Shigley, et al. (2006). Mechanical Engineering Design. The ninth edition, Mc Graw-Hill Book Company, New York.

[23] Ghafoori, E., Motavalli, M., Nussbaumer, A., Herwig, A., Prinz, G.S. & Fontana, M. (2015). Determination of minimum CFRP pre-stress levels for fatigue crack prevention in retrofitted metallic beams. *Engineering Structures*, *84*, 29-41.

[24] Sangid, M.D. (2013). The physics of fatigue crack initiation. *International journal of fatigue*, *57*, 58-72.

[25] Alizadeh, R., Marji, M. F., Abdollahipour, A. & Sagand, M. P. (2021). Development of higher-order displacement discontinuity method to simulate fatigue crack growth in brittle materials. *Engineering Fracture Mechanics*, *258*, 108087.

[26] Mughrabi, H. (2015). Microstructural mechanisms of cyclic deformation, fatigue crack initiation and early crack growth. *Philosophical Transactions of the Royal Society A: Mathematical, Physical and Engineering Sciences*, *373*(2038), 20140132

JOMAse | Received: 07-October-2022 | Accepted: 30-November-2023 | [(67) 3: 95-100]
Published by International Society of Ocean, Mechanical and Aerospace Scientists and Engineers, www.isomase.org., ISSN: 2354-7065 & e-ISSN: 2527-6085